Optically Transparent and Toughened Poly(methyl methacrylate) Composite Films with Acylated Cellulose Nanofibers

Naharullah Jamaluddin, Yu-I Hsu,* Taka-Aki Asoh, and Hiroshi Uyama*

Cite This: *ACS Omega* 2021, 6, 10752−10758

Read Online

ACCESS | Metrics & More | Article Recommendations | SI Supporting Information

ABSTRACT: In this work, nanocomposites of poly(methyl methacrylate) (PMMA) with cellulose nanofiber (CNF) were prepared by a solution casting technique. CNF was modified by propionic anhydride (PA) to form surface-propionylated CNF (CNFp) to improve its compatibility with the PMMA matrix. CNF, CNFp, and acetylated CNF were compared with respect to their influence as fillers in PMMA composite films by ultraviolet−visible transmittance, haze values, tensile strength testing, and water contact angle measurement. It was demonstrated that 1 wt % of CNFp has good compatibility and uniform dispersion in the PMMA matrix, as demonstrated by the formation of a smooth surface composite film with good transparency, enhanced tensile properties, improved toughness, and lower wettability. Therefore, PMMA/CNFp composite films have great potential for use in several applications such as lightweight transparent materials, window substitutes, and see-through packaging.
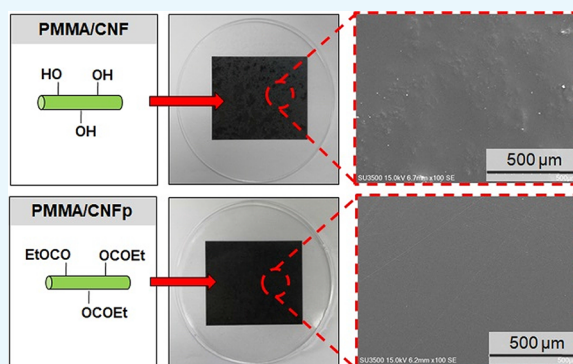
1. INTRODUCTION

In recent decades, various transparent polymers such as poly(methyl methacrylate) (PMMA), polystyrene (PS), and polycarbonate (PC) have gained attention because of their excellent optical clarity. As one of the transparent polymers, PMMA is an important material with good processability that has been used for several applications such as windows, lenses, and optical devices. Also, PMMA is often used as a substitute for glass material because of its high mechanical−dynamical properties and optical transparency. However, the applications of PMMA are limited owing to its insufficient mechanical strength and impact resistance, which limit its efficiency in engineering applications.[1] Therefore, some research has been conducted to overcome these limitations by preparing composites of PMMA via reinforcement with nanosized and microsized fibers.[2−4] Cellulose is a great candidate as a filler to counter the drawbacks of PMMA due to its high mechanical strength and biodegradability.[5]

Then, cellulose has been widely studied for use in composites and has been incorporated with various polymers such as polyurethane (PU), poly(ε-caprolactone) (PCL), poly(ethylene glycol) (PEG), PS, and polypropylene (PP).[6−9] Many attempts have been made to prepare PMMA composites with various types of cellulose. For instance, Erbas Kiziltas et al. prepared PMMA/cellulose composites by varying the type of cellulose (cellulose nanofiber (CNF), CNC, and bacterial cellulose (BC)) and studied their effect on the properties of the composites.[10] They managed to slightly improve the physical properties of PMMA; however, its transparency was significantly reduced even with the addition

of a low amount of fillers. In 2017, Anju and Narayanankutty tried to improve the adhesion of PMMA and microcrystalline cellulose (MCC) by adding bis-(3-triethoxysilylpropyl)-tetrasulfide as a coupling agent.[11] Due to chemically bonded PMMA and MCC, the physical properties were greatly improved; however, they did not mention the optical properties of the product.

There have been reports that the mechanical properties and transparency of composite materials can be enhanced with the introduction of cellulose nanomaterials (CNMs), such as CNF and cellulose nanowhiskers (CNW), compared to microscale cellulose.[12,13] However, hydrophilic CNMs as fillers aggregate in the hydrophobic polymer matrix, and then the transparency of the CNM composite is reduced. Therefore, it is necessary to overcome these drawbacks by chemically modifying the CNF itself to obtain new functional groups depending on its applications.[14−17] As an example, in 2015, Dong et al. covered CNF with surface carboxylic acid groups to improve its interfacial interaction with the PMMA matrix and produced a homogeneous dispersion of CNF in toughened PMMA nanocomposite films.[18] However, carboxylate species have higher interaction with water and easily form hydrogen bond.
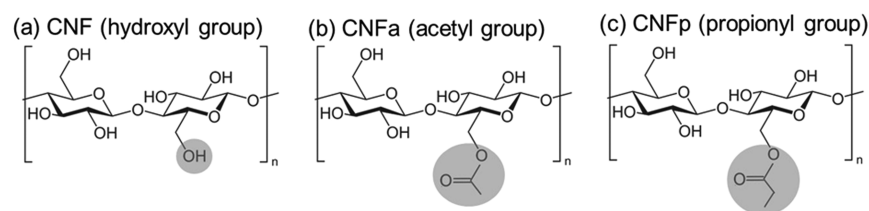
**Figure 1.** Chemical structures of (a) CNF, (b) CNFa, and (c) CNFp.

In other cases, the CNF was surface modified with polymerized methyl methacrylate (MMA) to prepare homogenized nano-composite with PMMA.[19] Acylation is another example of CNF modification that can alter its hydrophilicity and prevent the wetting behavior of CNF. Hence, it is expected to improve compatibility with hydrophobic polymer matrices. In the past year, research on thermoplasticization and acylation of several types of cellulose has been widely conducted by numerous methods, mainly for improving its water repellency without any specific applications.[20−22] However, very limited research has been reported on using acylated CNF as a reinforcement material in the PMMA matrix.

In this study, PMMA composites reinforced with surface-acylated CNF are presented. The objective of this work is to evaluate the dispersion improvement of CNF in the PMMA matrix while maintaining its high transparency by surface-modified CNF. Previously, we demonstrated that poly(lactic acid) (PLA) composites reinforced with surface-acetylated CNF (CNFa) show good mechanical strength and transparency due to the improvement of compatibility between PLA and CNF.[23] These results indicated that the acetyl group on the surface of the CNF improved the compatibility with the ester, and it is considered that it can be applied to PMMA. Here, CNFa and surface-propionylated CNFs (CNFp) were prepared and their dispersibility in PMMA was evaluated (Figure 1). The PMMA and CNFa composites were also expected to improve transparency, mechanical strength, and wettability. Comparing CNF, CNFa, and CNFp, aggregation was observed in CNF, whereas the dispersibility of CNFa and CNFp in PMMA was improved by surface modification. Furthermore, in the comparison between CNFa and CNFp, the hydrophobicity composites were improved using CNFp with a long alkyl chain length.

2. RESULTS AND DISCUSSION

2.1. Surface Modifications of CNF. Attenuated total reflection infrared (ATR-IR) was used to observe the substitution of acyl/acetyl groups at the hydroxyl groups of CNF after modification. Figure 2 shows a new peak appearing at around 1730 cm^{-1} after acylation by IR measurement, corresponding to the C=O stretching vibration modes of the carbonyl group between the CNF and propionic anhydride (PA). This indicates that the propionyl group from PA is incorporated into the CNF to become CNFp. Moreover, the change in the intensity of the carbonyl peaks based on different reaction times provides some insight into the acylation process. A longer reaction time produces a higher carbonyl peak intensity, which demonstrates that the acylation process increases with the reaction time.

2.2. Degree of Substitutions. Although the specific depth of modified CNFs is difficult to be acquired, SEM and electron-dispersive X-ray (EDX) analyses can estimate their depth. EDX spectroscopy showed a probed depth of 1−3 μm,
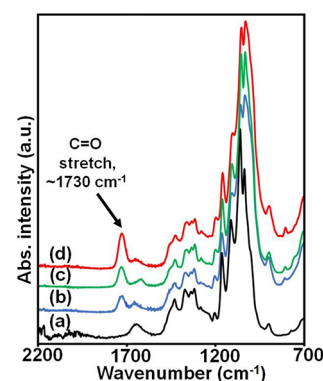
Figure 2. ATR-IR spectra of (a) CNF, (b) CNFp (1 h), (c) CNFp (2 h), and (d) CNFp (4 h).

while the average diameter of our CNF was about 69 ± 21 nm.[16] EDX indicates the composition of each element and therefore the degree of substitution (DS) of the CNF and modified CNF can be calculated. Based on this, the ratios of C and O of the CNF were 47.3% and 52.7%, respectively. As shown in Table 1, the CNF mass ratio from our study was very

Table 1. DS of CNFp Based on Reaction Time

species	mass concentration (%)		ratio (C:O)	modify % (DS)
	C	O		
CNF	47.7	52.3	0.91	0 (0)
CNFa	49.7	50.3	0.99	29.4 (0.88)[a]
CNFp (1 h)	51.2	48.8	1.05	20.8 (0.62)
CNFp (2 h)	52.5	47.5	1.11	30.7 (0.92)
CNFp (4 h)	55.0	45.0	1.22	51.8 (1.55)

[a]DS of CNFa is calculated using different equations due to its different molecular weights.

close to the theoretical value. Therefore, the results are significant for use in this study. After acylation, the ratio of C increased with an increase in the reaction time. The results showed that 51.8% acylation occurred with a DS of 1.55 after 4 h of the reaction time. There was an approximately 21.1% increase in acylation compared to that after 2 h of the reaction time. As expected, the 1 h reaction time had a lower DS (0.62), with only 20.8% of acylation occurring. The EDX results further confirm that the propionyl group was chemically bonded on the CNF and that the acylation increased with the reaction time.

2.3. Morphologies of PMMA Composites. CNF fillers resulted in different physical properties for the PMMA matrix in comparison with CNFa and CNFp fillers, especially on the surface, because of the differences in their compatibility. As shown in Figure 3a, the PMMA/CNF composite film has a rough surface, and it is clear that CNF fillers cause
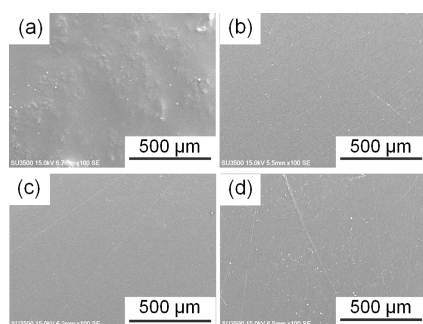
**Figure 3.** SEM images of (a) PMMA/CNF, (b) PMMA/CNFa, (c) PMMA/CNFp1, and (d) PMMA/CNFp2 composite films.

agglomeration on/in the PMMA matrix. Hence, the PMMA/CNF composite film shows a lumpy surface with clear white agglomerations. In contrast, the PMMA/CNFa composite film (Figure 3b) exhibits a flat and smooth surface, similar to that found in the PMMA/CNFp composite films with 1 wt % (Figure 3c) and 2 wt % (Figure 3d) CNFp. CNFa and CNFp were expected to have higher compatibility with PMMA owing to their hydrophobicity, while the hydrophilic CNF was expected to have less compatibility with PMMA. The scanning electron microscopy (SEM) images show that the CNFp filler is scattered on the surface but barely observed in the PMMA/CNFp1 composite film. This indicates that the compatibility between the PMMA matrix and CNFp filler is improved. The 2 wt % CNFp is more observable, mainly due to its higher concentration, which led to the agglomeration of the filler. Likewise, the CNFa filler scattered on the PMMA matrix is difficult to see in the PMMA/CNFa composite film. These results demonstrate that acetylation and acylation can change the compatibility of CNFs with the PMMA matrix. Thus, the agglomeration of CNFs can be avoided using CNFa or CNFp instead of unmodified CNFs.

2.4. Optical Transmittances of PMMA Composites.

Figure 4 shows the photographs of PMMA composite films with different concentrations and types of fillers. The patterns in the background can be observed clearly through the films, demonstrating that all films maintain the transparency of PMMA. However, the black-colored background clearly shows the white agglomeration of CNF fillers on the PMMA/CNF composite film (Figure 4b). Agglomeration of CNFa and CNFp in the matrix was confirmed to be minimal as the black background can still be observed clearly without any precipitation of fillers. Some white agglomerations observed on the PMMA/CNFp2 composite film (Figure 4e) are due to the high concentration of the CNFp filler. As previously mentioned, CNFa and CNFp have high compatibility with PMMA because of their similar hydrophobicity. For this reason, the PMMA/CNFa and PMMA/CNFp composite films have better transparency compared to the PMMA/CNF composite film.

2.5. Light Transmittances of PMMA Composites.

Ultraviolet−visible (UV−vis) spectroscopy was carried out to compare the transparency among PMMA composite films by calculating the percentage of UV−vis transmittance. The transmittance spectra of PMMA composite films in the visible wavelength region (400−800 nm) are shown in Figure 5. The average transmittance values, summarized in Table 2, were used as relative values for comparison. The neat PMMA film shows 79.6% transmittance, which is the highest among all the PMMA composite films. The heterogeneous nature of the PMMA/CNF composites reduces their transmittance to 66.2%, lower because of agglomeration, which results in the diffraction and scattering of light during UV−vis analysis. The composite films of PMMA with modified CNF fillers have better transmittances of 73.5% (CNFa), 71.6% (1 wt % CNFp), and 69.9% (2 wt % CNFp). These results can be
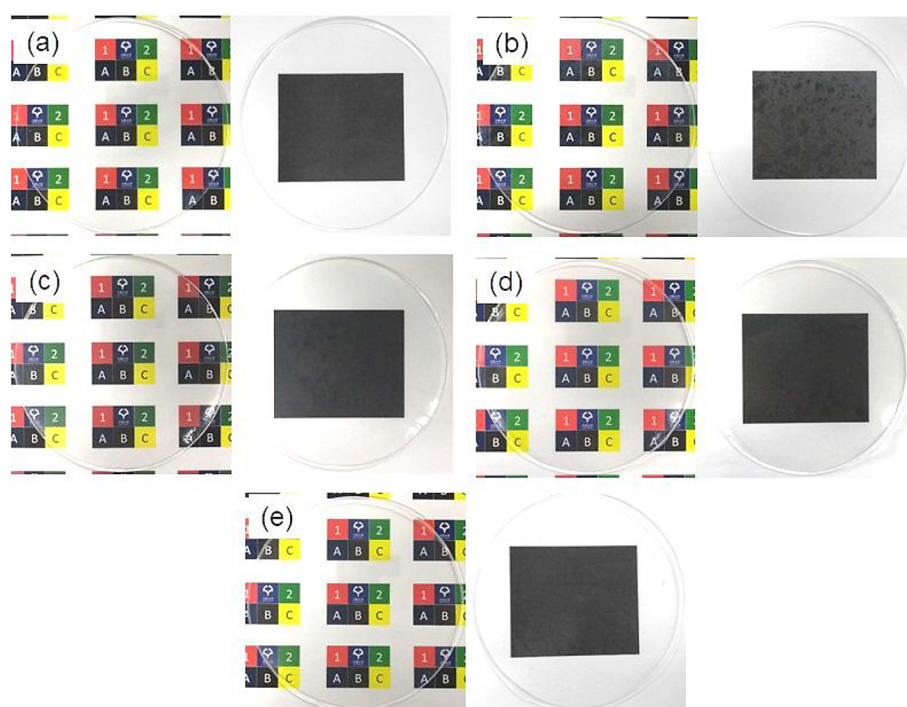
Figure 4. Photographs of (a) neat PMMA, (b) PMMA/CNF, (c) PMMA/CNFa, (d) PMMA/CNFp1, and (e) PMMA/CNFp2 composite films.
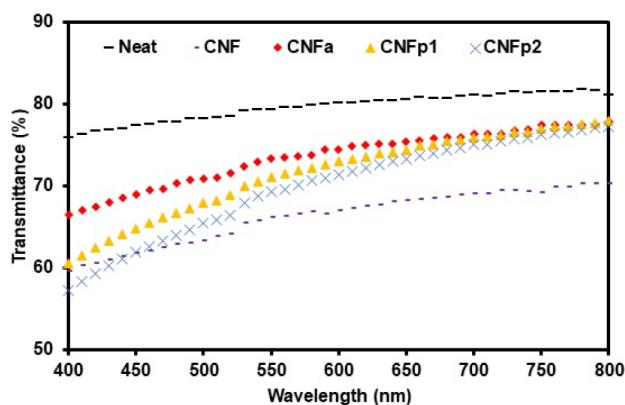
Figure 5. UV−vis transmittance of PMMA composite films.

Table 3. Average Tensile Strength, Young's Modulus, Average Elongation, and Toughness of PMMA Composite Films

composite films	tensile stress (MPa)	Young's modulus (GPa)	tensile strain (%)	toughness (×10³ kJ/mm³)
neat PMMA	33.1 ± 0.5	0.89 ± 0.13	3.8 ± 0.6	0.63 ± 0.01
PMMA/ CNF	31.3 ± 10.5	0.85 ± 0.09	3.8 ± 1.0	0.65 ± 0.44
PMMA/ CNFa	40.0 ± 7.7	1.04 ± 0.03	4.1 ± 0.8	1.12 ± 0.35
PMMA/ CNFp1	41.2 ± 2.9	1.26 ± 0.07	3.5 ± 0.2	1.02 ± 0.06
PMMA/ CNFp2	42.3 ± 5.9	1.08 ± 0.13	4.4 ± 0.9	1.39 ± 0.46

attributed to the better and uniform dispersion of the modified CNF in the PMMA matrix instead of the unmodified CNF.

2.6. Haze Transmittances of PMMA Composites. Table 2 summarizes the haze values, including the intensities of the whole transmitted light (T.T.) and parallel light (P.T.) of the PMMA composite films. Neat PMMA gave the lowest haze value among the films at 8.39%. After the addition of CNF fillers, the haze value increased to 25.5%. This is because the CNF fibers agglomerate during the composite film preparation, increasing the amount of reflected and scattered light. In comparison with the PMMA/CNF composite film, the haze values of the PMMA/CNFp composite films significantly decrease to 16.7% and 16.1% for 1 wt % and 2 wt % of CNFp, respectively. The compatibility and dispersion of the CNFp filler in the PMMA matrix are the key factors for achieving a lower haze value compared to the PMMA/CNF composite films. The PMMA/CNFa composite film shows a slightly lower haze value of 15.5% due to its better transparency. The film thickness was calculated to confirm its effect on the optical properties of the films. The results in Table 2 clearly show that thickness had no significant impact on the UV−vis transmittances or haze values.

2.7. Mechanical Properties of PMMA Composites. Table 3 shows the mechanical property values of the films, which are obtained from stress−strain curves (Figure S3). The neat PMMA film exhibits a tensile strength of 33.1 ± 0.5 MPa, and the CNF in the PMMA matrix does not cause any increase in tensile strength. The PMMA/CNF composite film's tensile strength is 31.3 ± 10.5 MPa owing to the incompatibility of PMMA and CNF, also indicated by the large standard deviation value. Certain regions in the film had lower tensile strength than neat PMMA, while other areas had higher values, confirming the inhomogeneity of the CNF in the PMMA matrix. In contrast, CNFa and CNFp in the PMMA matrix show an increase of approximately 20−28% compared to the neat PMMA because of better compatibility between the components. The tensile strength values for PMMA/CNFa,

PMMA/CNFp1, and PMMA/CNFp2 are 40.0 ± 7.7, 41.2 ± 2.9, and 42.3 ± 5.9 MPa, respectively. It is interesting to note that the tensile strength is increased slightly when CNFp2 is added compared to PMMA/CNFp1. This is because the higher concentration of CNFp leads to inhomogeneity of the filler with the PMMA matrix. Therefore, the increment recorded in PMMA/CNFp2 is lower by the less uniformity of the matrix and filler. In general, the product of solution casting possesses lower tensile strength compared to the melt blend method, which explains why the tensile strength of PMMA in this research is lower than that of pure commercialized or industrial PMMA.[24] The neat PMMA exhibits Young's modulus of 0.89 ± 0.13 GPa. Based on the same reason as that for tensile strength, the addition of the CNF filler slightly reduces the modulus to 0.85 ± 0.09 GPa, while CNFa and CNFp fillers enhance the modulus to 1.04 ± 0.03 and 1.26 ± 0.07 GPa, respectively. As for the strain to failure, the PMMA composite films show no significant difference in the strain percentage for all films, which ranges from 3.5% to 4.4% with a standard deviation of 0.2−1.0. Furthermore, the toughness of the neat PMMA film seems to increase by 78% when CNFa was added as a filler. PMMA/ CNFp1 and PMMA/CNFp2 composite films recorded an increment of 62% and 121%, respectively. It was proven that the compatibility of modified CNFs with the PMMA matrix leads to the increment of PMMA's toughness. However, the PMMA matrix with unmodified CNF fillers has no significant improvement in toughness.

2.8. Wettability of PMMA Composites. As summarized in Table 4, neat PMMA shows an average water contact angle (WCA) of 83.0°, whereas those of the PMMA/CNF composite film are 81.2°. It was demonstrated that CNF fillers have higher wettability due to CNF hydrophilicity. However, the CNFa and CNFp fillers have higher WCAs of 84.1°, 85.3°, and 86.2° for PMMA/CNFa, PMMA/CNFp1, and PMMA/CNFp2 composite films, respectively. These observations are attributed to a change from the hydrophilic

Table 2. Haze Values, Average Thickness, and Transmittances of PMMA Composite Films

composite films	transmitted light, T.T. (%)	parallel light, P.T. (%)	haze values (%)	average thickness (μm)	average transmittance (%)
Neat PMMA	91.9	83.7	8.9	235	79.6
PMMA/CNF	88.5	66.0	25.5	194	66.2
PMMA/CNFa	90.2	76.2	15.5	189	73.5
PMMA/CNFp1	90.2	75.2	16.7	206	71.6
PMMA/CNFp2	90.3	75.7	16.1	203	69.9

Table 4. Wettability of PMMA Composite Films

composite films	water contact angle (degree)
neat PMMA	83.0 ± 0.7
PMMA/CNF	81.2 ± 0.9
PMMA/CNFa	84.1 ± 3.4
PMMA/CNFp1	85.3 ± 0.4
PMMA/CNFp2	86.2 ± 1.0

CNF to the hydrophobic CNFa and CNFp. The substitution of acetyl and propionyl groups at the hydroxyl groups of the CNF is the main reason for this hydrophobicity. Hydrogen bonding of the CNF is reduced and hydroxyl groups are substituted by hydrophobic acetyl and propionyl groups. Therefore, the wettability of PMMA composite films can also be reduced by introducing hydrophobized CNF instead of unmodified CNF fillers. CNFp fillers provided slightly higher hydrophobicity than CNFa because the alkyl chain is slightly longer in the propionyl group of CNFp than in the acetyl group of CNFa, which slightly improves the hydrophobicity.

3. CONCLUSIONS

CNF was successfully modified into CNFp by substituting the hydroxyl group of CNF for a propionyl group from PA. By increasing the reaction time to 4 h, the DS of CNFp was improved to a value of 1.55 (51.8% acylation). PMMA composite films with CNF, CNFp, and CNFa as fillers were successfully fabricated by the solution casting technique. Comparison of transparency between composites with fillers showed that CNFp and CNFa have better compatibility with the PMMA matrix. The results obtained from images, UV−vis transmittance, and haze values confirmed that the PMMA matrix transparency was maintained. In comparison with neat PMMA and PMMA/CNF composite films, the mechanical properties of PMMA/CNFa and PMMA/CNFp were enhanced. The uniform dispersion of the CNFp and CNFa in the PMMA matrix is a key factor for this enhancement. Furthermore, the wettability of the PMMA composite films was reduced by the introduction of CNFp, resulting in a higher WCA for the PMMA/CNFp composite films. In general, the influence of CNFp and CNFa as fillers on the PMMA matrix was not very different and the transparency of the PMMA/CNFp composite films was slightly lower. Meanwhile, its mechanical and wettability properties were slightly enhanced compared to those of the PMMA/CNFa composite film. In conclusion, the incorporation of CNFp with PMMA improved the properties of the composite films, including transparency (compared with PMMA/CNF composite film), better mechanical properties, and lower wettability. Therefore, these newly developed PMMA composite films with PA-modified CNFs can serve as promising transparent reinforced plastic nanomaterials.

4. EXPERIMENTAL SECTION

4.1. Materials. MCC was obtained from Merck Japan Ltd. (Tokyo, Japan). *N,N*-Dimethylformamide (DMF) was purchased from Kanto Chemical (Tokyo, Japan). PA, acetic anhydride (AA), chloroform >99.0%, and acetone >99.0% were obtained from Wako Pure Chemical Industries (Osaka, Japan) and used without treatment. PMMA (M_w = 125,000) was purchased from Sigma-Aldrich (St. Louis, MO, USA). Water was treated using a model III instrument from Organo

Corporation (Tokyo, Japan) to produce deionized water (DI-H_2O).

4.2. Fibrillation of MCC. Fibrillation of MCC was conducted using a stone grinding machine (Masuko Sangyo, Saitama, Japan) without other chemical treatments. Details on the fibrillation of MCC to form CNFs are reported in our previous work.[16] Briefly, MCC (40 g) was soaked and stirred in water for 2 days to produce a suspension of 2 wt % MCC. Then, the MCC suspension was ground at 1500 rpm for five cycles with a stone grinder grit size of 80 (ultrafine). MCC automatically exited the chute as the fiber size decreased, in the form of CNF. Each cycle was repeated when the hopper was almost empty by transferring the product of the previous cycle back into the hopper. After five cycles, the suspension of CNF (1.57 wt %) in water was stored in a glass bottle and kept in a refrigerator (<4 °C).

4.3. Surface Modification of CNF. First, 0.81 g of CNF in water (1.57 wt %) was homogenized with 80 mL of DMF. The CNF suspension in this mixed solvent was transferred to a rotary evaporator to remove the water from the system. The mixture was then transferred into a round-bottomed flask connected to a reflux condenser, on a hotplate heated to 110 °C using silicon oil, and simultaneously, PA (0.5 mol) was added. The acylation reaction time was varied from 1 to 4 h to study the acylation process. Then, the solution was quenched in an ice bath followed by the addition of acetone (50 mL). The solution was then centrifuged and washed several times with acetone to remove unreacted chemicals and DMF. Finally, the medium was exchanged with chloroform to obtain CNFp in chloroform. The products were stored in a refrigerator (<4 °C) before the preparation of the PMMA composite films. For CNFa, PA was substituted with AA and the acetylation process duration was fixed at 4 h.

4.4. Preparation of PMMA Composites. The solution casting method was used to prepare PMMA composites. First, a dispersion of CNF, CNFa, or CNFp in chloroform (0.02 g or 0.04 g of solid content for 1 wt % or 2 wt %, respectively) was poured into a beaker, and chloroform was added to reach 50 g in total weight. Next, 2 g of PMMA were added and the mixture was stirred for 1 h at room temperature. The mixture was then poured into a Petri dish and left overnight in a bioshaker at 25 rpm and 40 °C to evaporate the chloroform. The samples were denoted as neat PMMA (without filler), PMMA/CNF, PMMA/CNFp, and PMMA/CNFa composite films. Throughout this study, CNFp and CNFa with a 4 h reaction time were used as fillers. Also, preparation of the film using CNF without the PMMA matrix will form fiber aggregates, instead of a film due to the incompatibility between CNF and chloroform.

4.5. Characterizations. An ATR-IR instrument (iD5 ATR, Thermo Scientific, Waltham, MA, USA) was used to observe functional groups after modification. EDX spectroscopy was carried out to calculate the DS of CNFp produced using a Miniscope TM3000/SwiftED3000, Hitachi, Tokyo, Japan. For the DS calculation in this research, C and O elements, but not H, were included. After acylation, the mass ratio of C was expected to increase relative to O due to increased C species from the propionyl groups that substitute for H in the hydroxyl groups of CNF (Figure S1). Equations 1 and 2 were derived and further used for the calculations:

$$A = \frac{200(10B - 9)}{3(9 - 4B)} \tag{1}$$

$$DS = \frac{A}{100} \times 3 \qquad (2)$$

where A is the percentage of acylation (%) and B is the mass ratio of C to O (C:O) for CNFp. The derivations for eqs 1 and 2 are shown in eq S1. The morphology of the PMMA composite films was observed with an SEM instrument (SU3500, Hitachi, Tokyo, Japan) using an Au−Pd sputter to increase the sample's surface conductivity. The samples were cut and attached to circular SEM plates (25 cm). For surface morphology, magnification at 100× (500 μm scale) was used to provide a wide area of the film's surface. The transmittance of the composite films was determined using a UV−vis spectrophotometer (U-2810 spectrophotometer, Hitachi, Tokyo, Japan) in the visible region (200−800 nm) scanned at a rate of 800 nm/min. A haze meter (NDH 4000, Nippon Denshoku) was employed to calculate the haze values of the PMMA composite films. The haze value was measured using eq 3:

$$Haze = \frac{T.T. - P.T.}{T.T.} \times 100 \qquad (3)$$

The mechanical properties of the composite films were investigated using a universal testing machine (EZ Graph, Shimadzu, Kyoto, Japan) following the JIS K6251-8 standard. Each sample was cut into dumbbell shapes for at least five tests and dried in an oven at 80 °C before analysis to remove any remaining solvent and moisture. The crosshead speed was 50 mm/min with a load cell of 100 N. Tensile toughness was also measured by calculating the area under stress−strain curves (Figure S3). The wettability of the films was studied with a WCA test using a Drop Master DM300, Kyowa Interface Science, Tokyo, Japan, with the FAMAS basic software. Each sample was dried in an oven at 80 °C before analysis, measured for at least six specimens, and four of the least deviated values were used to calculate the average WCA.

■ ASSOCIATED CONTENT

Ⓢ Supporting Information

The Supporting Information is available free of charge at https://pubs.acs.org/doi/10.1021/acsomega.1c00325.

Chemical equation of the acylation process of CNF into CNFp; ATR-IR spectra of CNF, CNFp1, CNFp2, and CNFp4; derivation of equation from EDX analysis for DS calculation; and stress−strain curve from tensile test to calculate tensile toughness (PDF)

■ AUTHOR INFORMATION

Corresponding Authors

Yu-I Hsu − *Department of Applied Chemistry, Graduate School of Engineering, Osaka University, Suita, Osaka 565-0871, Japan;* ⓞ orcid.org/0000-0002-4533-7200; Email: yuihsu@chem.eng.osaka-u.ac.jp

Hiroshi Uyama − *Department of Applied Chemistry, Graduate School of Engineering, Osaka University, Suita, Osaka 565-0871, Japan;* ⓞ orcid.org/0000-0002-8587-2507; Phone: +81-6-6879-7364; Email: uyama@chem.eng.osaka-u.ac.jp; Fax: +81-6-6879-7367

Authors

Naharullah Jamaluddin − *Department of Applied Chemistry, Graduate School of Engineering, Osaka University, Suita, Osaka 565-0871, Japan*

Taka-Aki Asoh − *Department of Applied Chemistry, Graduate School of Engineering, Osaka University, Suita, Osaka 565-0871, Japan;* ⓞ orcid.org/0000-0001-9087-5174

Complete contact information is available at:
https://pubs.acs.org/10.1021/acsomega.1c00325

Author Contributions

Photos in this manuscript, Table of Contents, and Supporting Information were obtained, captured, or edited by N.J. All authors are working in the same laboratory.

Notes

The authors declare no competing financial interest.

■ REFERENCES

(1) Liu, H.; Liu, D.; Yao, F.; Wu, Q. Fabrication and Properties of Transparent Polymethylmethacrylate/Cellulose Nanocrystals Composites. *Bioresour. Technol.* **2010**, *101*, 5685−5692.

(2) Nussbaumer, R. J.; Caseri, W. R.; Smith, P.; Tervoort, T. Polymer-TiO₂ Nanocomposites: A Route towards Visually Transparent Broadband UV Filters and High Refractive Index Materials. *Macromol. Mater. Eng.* **2003**, *288*, 44−49.

(3) Chen, L.-S.; Huang, Z.-M.; Dong, G.-H.; He, C.-L.; Liu, L.; Hu, Y.-Y.; Li, Y. Development of a Transparent PMMA Composite Reinforced with Nanofibers. *Polym. Compos.* **2009**, *30*, 239−247.

(4) Tang, E.; Cheng, G.; Ma, X. Preparation of Nano-ZnO/PMMA Composite Particles via Grafting of the Copolymer onto the Surface of Zinc Oxide Nanoparticles. *Powder Technol.* **2006**, *161*, 209−214.

(5) Shalwan, A.; Yousif, B. F. In State of Art: Mechanical and Tribological Behaviour of Polymeric Composites Based on Natural Fibres. *Mater. Des.* **2013**, *48*, 14−24.

(6) Pei, A.; Malho, J. M.; Ruokolainen, J.; Zhou, Q.; Berglund, L. A. Strong Nanocomposite Reinforcement Effects in Polyurethane Elastomer with Low Volume Fraction of Cellulose Nanocrystals. *Macromolecules* **2011**, *44*, 4422−4427.

(7) Goffin, A. L.; Raquez, J. M.; Duquesne, E.; Siqueira, G.; Habibi, Y.; Dufresne, A.; Dubois, P. Poly(ε-Caprolactone) Based Nanocomposites Reinforced by Surface-Grafted Cellulose Nanowhiskers via Extrusion Processing: Morphology, Rheology, and Thermo-Mechanical Properties. *Polymer (Guildf)* **2011**, *52*, 1532−1538.

(8) Lin, N.; Dufresne, A. Physical and/or Chemical Compatibilization of Extruded Cellulose Nanocrystal Reinforced Polystyrene Nanocomposites. *Macromolecules* **2013**, *46*, 5570−5583.

(9) Iwamoto, S.; Yamamoto, S.; Lee, S. H.; Endo, T. Mechanical Properties of Polypropylene Composites Reinforced by Surface-Coated Microfibrillated Cellulose. *Composites, Part A* **2014**, *59*, 26−29.

(10) Erbas Kiziltas, E.; Kiziltas, A.; Bollin, S. C.; Gardner, D. J. Preparation and Characterization of Transparent PMMA-Cellulose-Based Nanocomposites. *Carbohydr. Polym.* **2015**, *127*, 381−389.

(11) Anju, V. P.; Narayanankutty, S. K. Impact of Bis-(3-Triethoxysilylpropyl)Tetrasulphide on the Properties of PMMA/Cellulose Composite. *Polymer (Guildf)* **2017**, *119*, 224−237.

(12) Jonoobi, M.; Aitomäki, Y.; Mathew, A. P.; Oksman, K. Thermoplastic Polymer Impregnation of Cellulose Nanofibre Networks: Morphology, Mechanical and Optical Properties. *Composites, Part A* **2014**, *58*, 30−35.

(13) Wang, D.; Yu, J.; Zhang, J.; He, J.; Zhang, J. Transparent Bionanocomposites with Improved Properties from Poly(Propylene Carbonate) (PPC) and Cellulose Nanowhiskers (CNWs). *Compos. Sci. Technol.* **2013**, *85*, 83−89.

(14) Klemm, D.; Kramer, F.; Moritz, S.; Lindström, T.; Ankerfors, M.; Gray, D.; Dorris, A. Nanocelluloses: A New Family of Nature-Based Materials. *Angew. Chem., Int. Ed. Engl.* **2011**, *50*, 5438−5466.

(15) Foster, E. J.; Moon, R. J.; Agarwal, U. P.; Bortner, M. J.; Bras, J.; Camarero-Espinosa, S.; Chan, K. J.; Clift, M. J. D.; Cranston, E. D.; Eichhorn, S. J.; Fox, D. M.; Hamad, W. Y.; Heux, L.; Jean, B.; Korey, M.; Nieh, W.; Ong, K. J.; Reid, M. S.; Renneckar, S.; Roberts, R.; Shatkin, J. A.; Simonsen, J.; Stinson-Bagby, K.; Wanasekara, N.; Youngblood, J. Current Characterization Methods for Cellulose Nanomaterials. *Chem. Soc. Rev.* **2018**, *47*, 2609−2679.

(16) Jamaluddin, N.; Kanno, T.; Asoh, T.-A.; Uyama, H. Surface Modification of Cellulose Nanofiber Using Acid Anhydride for Poly(Lactic Acid) Reinforcement. *Mater. Today Commun.* **2019**, *21*, No. 100587.

(17) Habibi, Y. Key Advances in the Chemical Modification of Nanocelluloses. *Chem. Soc. Rev.* **2014**, *43*, 1519−1542.

(18) Dong, H.; Sliozberg, Y. R.; Snyder, J. F.; Steele, J.; Chantawansri, T. L.; Orlicki, J. A.; Walck, S. D.; Reiner, R. S.; Rudie, A. W. Highly Transparent and Toughened Poly(Methyl Methacrylate) Nanocomposite Films Containing Networks of Cellulose Nanofibrils. *ACS Appl. Mater. Interfaces* **2015**, *7*, 25464−25472.

(19) Shih, Y. F.; Chou, M. Y.; Lian, H. Y.; Hsu, L. R.; Chen-Wei, S. M. Highly Transparent and Impact-Resistant PMMA Nanocomposites Reinforced by Cellulose Nanofibers of Pineapple Leaves Modified by Eco-Friendly Methods. *Express Polym. Lett.* **2018**, *12*, 844−854.

(20) Huang, L.; Wu, Q.; Wang, Q.; Wolcott, M. One-Step Activation and Surface Fatty Acylation of Cellulose Fibers in a Solvent-Free Condition. *ACS Sustainable Chem. Eng.* **2019**, *7*, 15920−15927.

(21) Gorade, V. G.; Kotwal, A.; Chaudhary, B. U.; Kale, R. D. Surface Modification of Microcrystalline Cellulose Using Rice Bran Oil: A Bio-Based Approach to Achieve Water Repellency. *J. Polym. Res.* **2019**, *26*, 1−12.

(22) Miyagi, K.; Teramoto, Y. Function Extension of Dual-Mechanochromism of Acylated Hydroxypropyl Cellulose/Synthetic Polymer Composites Achieved by "Moderate" Compatibility as Well as Hydrogen Bonding. *Polymer (Guildf)* **2019**, *174*, 150−158.

(23) Jamaluddin, N.; Kanno, T.; Asoh, T. A.; Uyama, H. Surface Modification of Cellulose Nanofiber Using Acid Anhydride for Poly(Lactic Acid) Reinforcement. *Mater. Today Commun.* **2019**, *21*, No. 100587.

(24) Varela-Rizo, H.; Bittolo-Bon, S.; Rodriguez-Pastor, I.; Valentini, L.; Martin-Gullon, I. Processing and Functionalization Effect in CNF/PMMA Nanocomposites. *Composites, Part A* **2012**, *43*, 711−721.